

Endothelin-1 Receptor Blockade Prevented the Electrophysiological Dysfunction in Cardiac Myocytes of Streptozotocin-Induced Diabetic Rats

Yanfeng Ding, Ruijiao Zou, Robert L. Judd, and Juming Zhong

Department of Anatomy, Physiology and Pharmacology, College of Veterinary Medicine, Auburn University, Auburn, AL

Diabetes mellitus is complicated with the development of cardiac contractile dysfunction and electrical instability, which contributes to high morbidity and mortality in diabetic patients. This study examined the possible roles of enhanced endothelin-1 (ET-1) on diabetes-induced alterations in ventricular myocyte electrophysiology. Type 1 diabetic rats were induced by single dose injection of streptozotocin (STZ) and treated with or without ET-1 receptor antagonist bosentan for 8 wk before myocyte isolation. Action potential, outward K^+ currents, and inward Ca^{2+} currents in ventricular myocytes were recorded using whole-cell patch clamp technique. STZ-injected rats exhibited hyperglycemia, reduced body weight gain, and elevated plasma ET-1 concentration, indicative of diabetes induction. Ventricular myocytes isolated from diabetic rats exhibited prolonged action potential and reduced all three types of outward K^+ currents. Resting membrane potential, height of action potential, and L-type Ca^{2+} current were not altered in diabetic myocytes. In vivo chronic treatment of diabetic rats with bosentan significantly augmented K^+ currents and reversed action potential prolongation in ventricular myocytes. On the other hand, bosentan treatment had no detectable effect on the electrophysiological properties in control myocytes. In addition, bosentan had no effect on L-type Ca^{2+} currents in both control and diabetic myocytes. Our data suggest that altered electrophysiological properties in ventricular myocytes were largely resulted from augmented ET-1 system in diabetic animals.

Key Words: Diabetic cardiomyopathy; endothelin-1; bosentan; action potential; K^+ channels.

Introduction

Cardiovascular complications are main causes of morbidity and mortality in both human diabetic patients and experimental diabetes mellitus. There are distinct alter-

ations in structure, mechanical, and electrophysiological properties of the diabetic myocardium (1–4). The most prominent electrophysiological change is the prolongation of the Q-T interval due to an increase in ventricular action potential duration (APD) (5–10). The ionic mechanisms underlying AP prolongation in diabetic animals have been attributed to the downregulation of outward K^+ currents, including the transient outward current I_{to} , the delayed rectifying outward current I_k , and the instantaneous, non-inactivating steady-state current I_{ss} (5,7,8,11,12). However, little is known regarding the mechanism(s) underlying the ion channel abnormalities associated with clinical prolongation of the Q-T interval in diabetic patients.

Recent studies suggest that endothelin-1 (ET-1) may play an important role in the functional and structural changes in diabetes-induced cardiovascular dysfunction. Elevated levels of plasma ET-1, and increased tissue mRNA expression for ET-1, ET-3, and both ET and ET receptors, have also been observed in human diabetic patients as well as in various animal models of diabetes (1,13–15). Long-term treatment with ET-1 receptor antagonists limited diabetes-induced development of focal myocardial fibrosis and improved in vivo ventricular function in diabetic rats (1,13,16). Furthermore, our recent study demonstrates that in vivo treatment of diabetic rats with ET-1 receptor antagonist, bosentan, reversed diabetes-induced myocyte contractile dysfunction (17). Nevertheless, no study has addressed the possible roles of enhanced ET system in the diabetes-induced cardiac electrophysiological abnormalities. The primary aim of the present study was to determine the possible roles of enhanced ET-1 in diabetes-induced downregulation of K^+ channel activity in ventricular myocytes. To answer this question, we recorded ionic currents and membrane potentials in ventricular myocytes isolated from control and diabetic rats treated with and without ET-1 receptor antagonist, bosentan.

Results

General Characteristics of Experimental Animals

Rats injected with STZ exhibited the characteristic symptoms of uncontrolled diabetes including hyperglycemia, polyuria, decreased body weight gain, polydipsia, and polyphagia compared to age-matched controls. Control animals

Received March 16, 2006; Revised April 21, 2006; Accepted June 26, 2006.
Author to whom all correspondence and reprint requests should be addressed:
Juming Zhong, DVM, PhD, Department of Anatomy, Physiology and Pharmacology, Auburn University, College of Veterinary Medicine, Auburn, AL 36849. E-mail: zhongju@auburn.edu

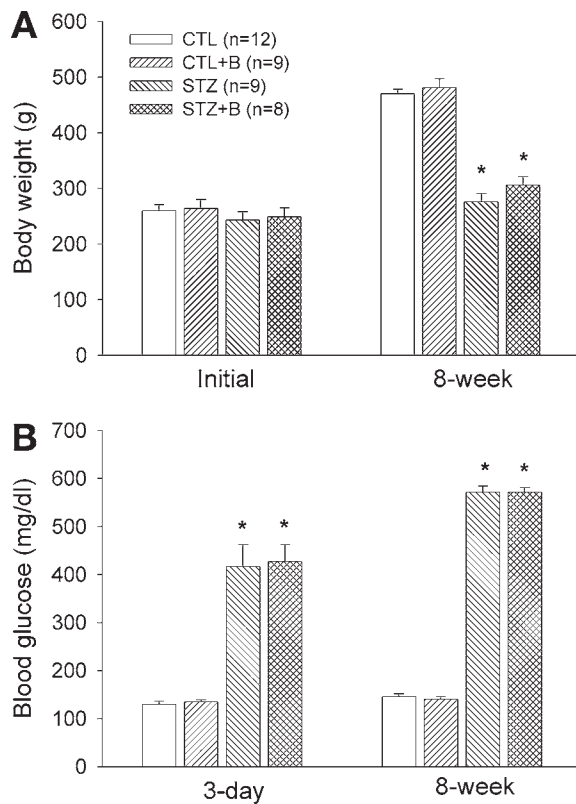


Fig. 1. Effect of bosentan treatment on body weight (A) and blood glucose levels (B) in control and diabetic rats. Values are means \pm SE. CTL: control rats, CTL+B: control rats treated with bosentan, STZ: streptozotocin-induced diabetic rats, STZ+B: diabetic rats treated with bosentan. *represents significantly different from the values of the control counterparts ($p < 0.05$).

showed a significant gain of body weight and a stable level of blood glucose throughout the 8-wk experimental period. In rats injected with STZ, plasma glucose levels were significantly elevated (>350 mg/dL) as early as 2 d post-injection and remained elevated throughout the 8-wk experimental period. Body weight gain of STZ-injected rats was dramatically reduced. Thus, all STZ-injected rats were considered diabetic and included in the experiments. Bosentan treatment had no effect on those parameters in both control and diabetic animals. These data are summarized in Fig. 1.

Effects of Bosentan on Membrane Potentials in Ventricular Myocytes

The morphology of action potentials was clearly changed in myocytes isolated from both groups of diabetic rats compared with control rats. Neither the resting membrane potentials nor the action potential amplitudes differed among four experimental groups of animals. Resting membrane potentials were -65 ± 1 mV, -68 ± 1 mV, -66 ± 1 mV and -66 ± 2 mV, respectively, and the amplitudes of action potential were 94 ± 4 mV, 93 ± 3 mV, 92 ± 5 mV, and 98 ± 4 mV, respectively, for myocytes obtained from control rats ($n = 12$), control rats treated with bosentan ($n = 9$), diabetic rats ($n = 9$), and diabetic rats treated with bosentan ($n =$

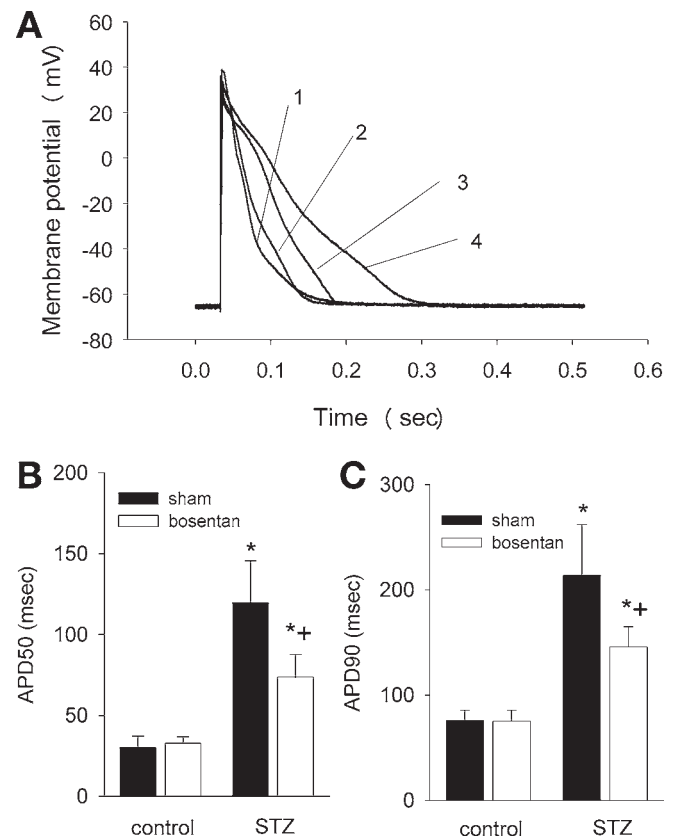


Fig. 2. Effect of bosentan treatment on action potentials in ventricular myocytes obtained from control and diabetic rats. (A) Superimposed action potential recordings in myocytes isolated from control (1), control treated with bosentan (2), diabetic (4), and diabetic rat treated with bosentan (3). Myocytes were superfused with normal Tyrode's solution (1.8 mM Ca^{2+}). Action potentials were elicited by applying a 6–10 ms current pulse (30% above the threshold) and recorded 3 min after whole-cell configuration. (B) Averaged times to 50% (APD50) and 90% (APD90) repolarization. Three to five myocytes were tested from each animal and data averaged to represent that animal. Data represent means \pm SE for control rats ($n = 12$), control rats treated with bosentan ($n = 9$), diabetic rats ($n = 9$), and diabetic rats treated with bosentan ($n = 8$). *represents significantly different from the control values and +represents significantly different from values taken from the non-treated diabetic rats ($p < 0.05$).

8). However, the action potential duration (APD) of diabetic myocytes was significantly longer than that of control myocytes. The times to 50% repolarization and 90% repolarization were increased 300% and 200%, respectively, in diabetic myocytes when compared with control values (Fig. 2). In vivo ET-1 receptor blockade using bosentan did not affect any parameters of action potential in myocytes obtained from control rats, but significantly reduced the prolongation of APD in diabetic myocytes (Fig. 2).

Effects of Bosentan on Membrane Currents in Ventricular Myocytes

The action potential duration is mainly determined by transmembrane Ca^{2+} influx through L-type Ca^{2+} channels and K^{+} outflow through different K^{+} channels (18). Thus

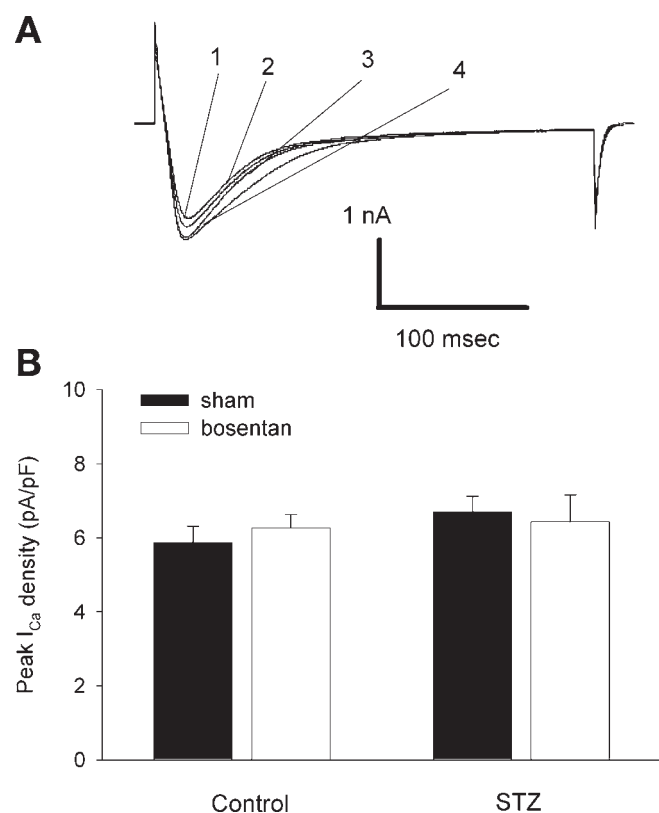


Fig. 3. Effect of bosentan treatment on L-type Ca²⁺ currents in ventricular myocytes obtained from control and diabetic rats. (A) Superimposed Ca²⁺ current recordings in myocytes isolated from control (1), control treated with bosentan (2), diabetic (3), and diabetic rat treated with bosentan (4). Inward currents were elicited by stepping the membrane potential to +10 mV from the holding potential of -40 mV and recorded 3 min after whole-cell configuration. (B) Averaged Ca²⁺ current densities in different groups of myocytes. Three to five myocytes were tested from each animal and data averaged to represent that animal. Peak current was divided with the cell capacitance to calculate the peak current density in each cell (pA/pF). Data represent means \pm SE for control rats ($n = 12$), control rats treated with bosentan ($n = 9$), diabetic rats ($n = 9$), and diabetic rats treated with bosentan ($n = 8$). There is no significant difference among the values from different groups of animals.

we compared both inward Ca²⁺ currents and outward K⁺ currents in ventricular myocytes from different groups of animals. Figure 3 shows the superimposed current recordings and averaged I_{CaL} densities in myocytes obtained from different groups of animals. L-type Ca²⁺ channel activity in ventricular myocytes was not altered by induction of diabetes. In addition, bosentan treatment did not have any effect on Ca²⁺ channel activity in myocytes obtained from either control or diabetic rats. The averaged peak current densities and the rates of current decay were not significantly different among all groups of animals. In contrast, all three types of outward K⁺ currents tested in our studies were significantly depressed in diabetic rat hearts. Figure 4 illustrates the samples of K⁺ current recordings and averaged current density–voltage relationships of I_{to}, I_k, and I_{ss}

recorded in ventricular myocytes taken from four groups of rats. The current amplitudes and densities of I_{to}, I_k, and I_{ss} were significantly lower in diabetic myocytes at test potentials ranging from -20 to +60 mV, compared to the values of control myocytes. In vivo bosentan treatment of diabetic animals significantly enhanced all three types of K⁺ currents in ventricular myocytes. On the other hand, bosentan treatment did not alter K⁺ channel activities in myocytes obtained from control rats.

Effects of Bosentan on Diabetes-Induced Myocyte Arrhythmic Contraction

Cardiac electrical instability often results in myocyte arrhythmic contraction. To test the hypothesis that ET-1 receptor blockade may reduce diabetes-induced ventricular arrhythmia, we measured the occurrence of arrhythmic contractions in ventricular myocytes isolated from rats treated with or without bosentan treatment. Myocyte contraction was elicited by field stimulation at 1 Hz frequency. Figure 5A shows the representative traces of intracellular Ca²⁺ fluctuation and sarcomere length change during stimulated contraction and occurrence of spontaneous contraction in a ventricular myocyte isolated from a diabetic rat. Figure 5B illustrates the averaged fractional occurrence of myocyte spontaneous contraction, or arrhythmic contraction, in all groups of animals tested. In both bosentan-treated and non-treated control groups, the occurrence of arrhythmic contraction was below 5%. On the other hand, more than 35% of myocytes obtained from diabetic rat without bosentan treatment demonstrated spontaneous contraction. In vivo treatment of diabetic rats with bosentan significantly reduced the arrhythmic contraction in ventricular myocytes.

Discussion

The primary observations in the present study include that (1) chronic diabetes induced by STZ injection significantly prolonged the action potential duration that were associated with profound reduction in outward K⁺ currents (I_{to}, I_k, and I_{ss}) in rat ventricular myocytes; (2) there is high incidence of myocyte arrhythmic contraction in diabetic rats; and (3) in vivo treatment of diabetic rats with ET-1 receptor antagonist, bosentan, significantly prevented diabetes-induced alterations of action potential and outward K⁺ currents, as well as reduced the occurrence of arrhythmic contraction in ventricular myocytes. On the other hand, L-type Ca²⁺ current density was not changed in ventricular myocytes from diabetic rats. In vivo treatment of control rats with bosentan had no detectable effect on electrophysiological properties in normal ventricular myocytes. Our present study is the first to demonstrate the beneficial effect of ET-1 antagonism on diabetes-induced alteration in cardiac electrophysiological properties at single cell level. Our data clearly show that enhanced ET-1 in streptozotocin-induced diabetes mellitus plays an important role in cardiac electrical instability observed in diabetic patients and poten-

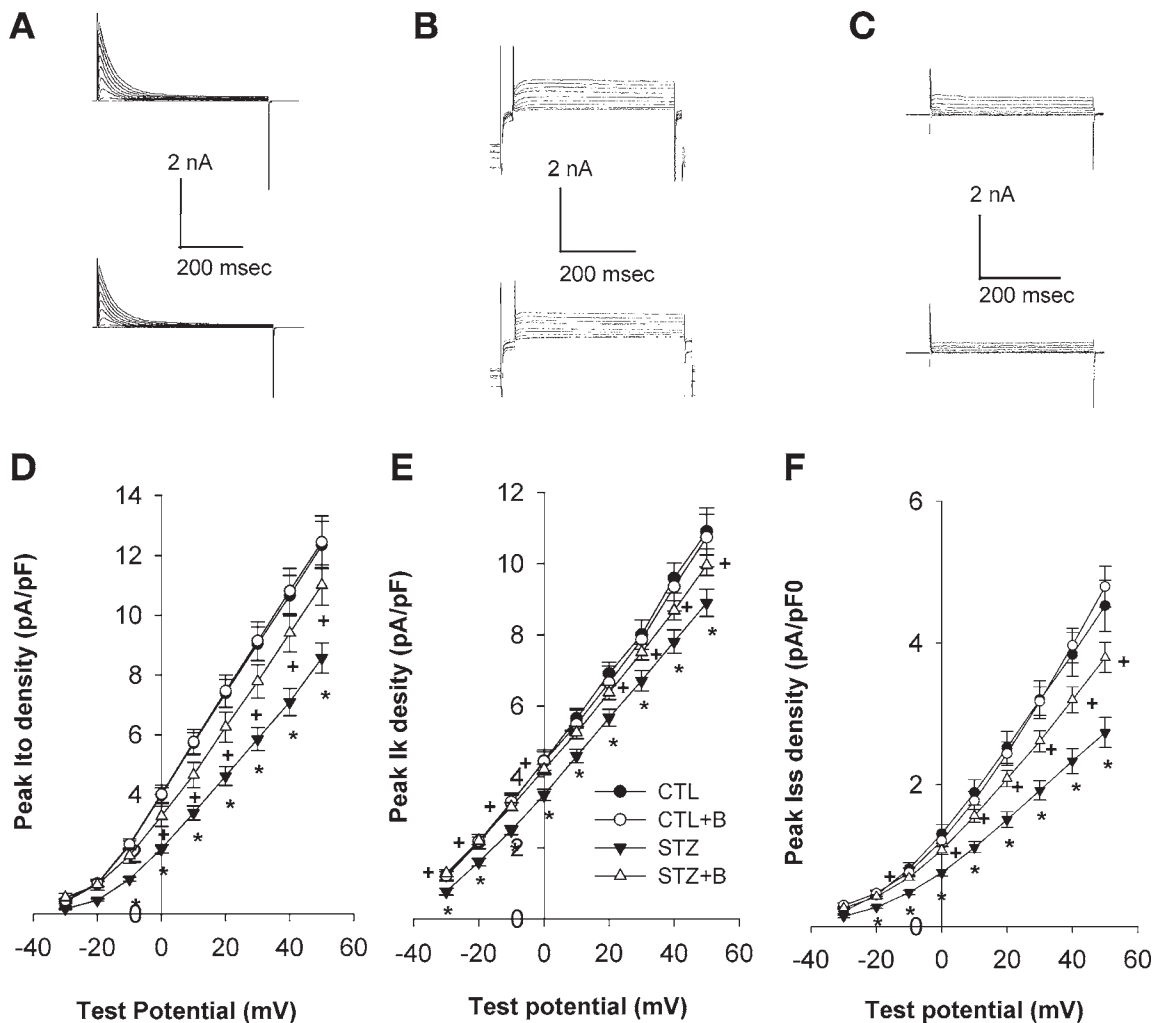


Fig. 4. Effect of bosentan treatment on outward K^+ currents in ventricular myocytes obtained from control and diabetic rats. **A**, **B**, and **C** show the representative recordings for I_{to} , I_k , and I_{ss} , respectively, in control myocytes (top), and diabetic myocytes (bottom). Currents were recorded 3 min after whole-cell configuration using different protocols (see Methods). **(D)** Averaged I_{to} density-voltage relationships. **(E)** Averaged I_k density-voltage relationships. **(F)** Averaged I_{ss} density-voltage relationships. Three to five myocytes were tested from each animal and data averaged to represent that animal. Peak current was divided with the cell capacitance to calculate the peak current density in each cell (pA/pF). Data represent means \pm SE for control rats (CTL, $n = 12$), control rats treated with bosentan (CTL+B, $n = 9$), diabetic rats (STZ, $n = 9$), and diabetic rats treated with bosentan (STZ+B, $n = 8$). *represents significantly different from the control values and +represents significantly different from values taken from the non-treated diabetic rats ($p < 0.05$).

tial therapeutic application of ET-1 receptor antagonism in the treatment of diabetic-induced cardiac complications.

Associated with mechanical and biochemical changes in diabetic cardiomyopathy, the most prominent and lethal electrophysiological alteration in diabetic patients is a prolonged Q-T dispersion due to an increase of cardiac action potential duration (19–21). The molecular basis for the electrophysiological changes observed in diabetic animal models has been attributed to downregulation of outward K^+ channel activity, including the transient outward current I_{to} , the delayed rectifying outward current I_k , and the steady-state outward current I_{ss} (5,22–25). Associated with the depression of the currents, mRNA and protein expression levels of Kv4.2 and Kv1.2 that underlie I_{to} and I_{ss} were dramatically lower in diabetic rat myocytes compared to that in control rat myocytes (24,26). Results from our pres-

ent study demonstrate that all three types of K^+ currents were significantly depressed in diabetic ventricular myocytes. Depressed K^+ currents were associated with prolonged action potential duration and frequent occurrence of myocyte arrhythmic contraction. Furthermore, our data provide evidence to suggest the important role of enhanced ET-1 in the diabetes-induced cardiac electrophysiological changes, as in vivo treatment with ET-1 receptor blockade bosentan restored diabetes-induced alterations in ventricular APD and outward K^+ currents as well as reduced diabetes-induced myocyte arrhythmic contraction.

There is growing evidence that ET-1 is involved in the progressive deterioration of cardiac contractile function in diabetic patients and animal models. Plasma ET-1 concentrations are elevated in the diabetic patient (1,14,27) and experimental models of diabetic animals (15,28). Upregu-

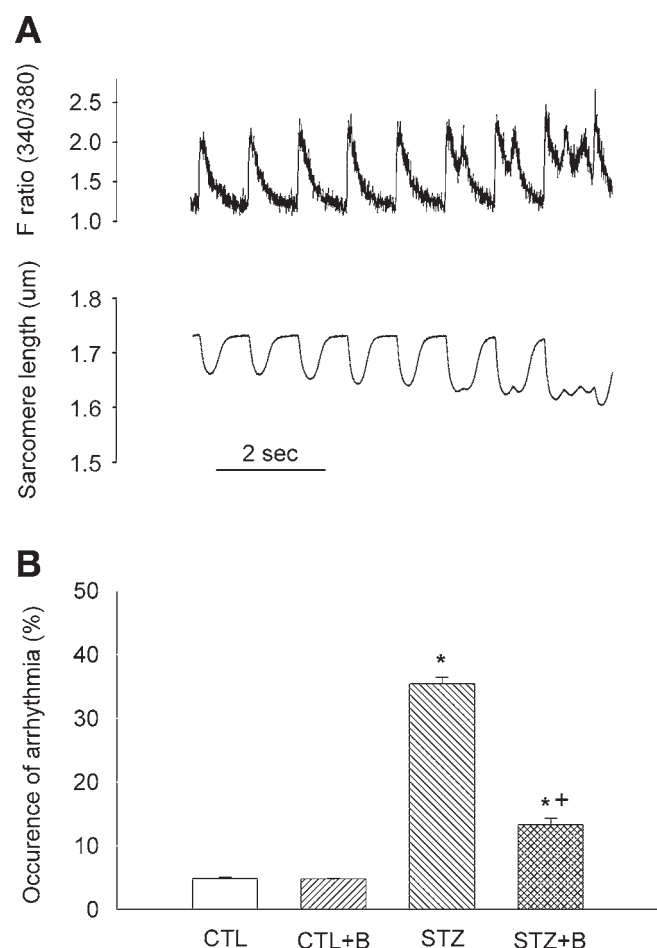


Fig. 5. Effect of bosentan treatment on occurrence of spontaneous contraction in ventricular myocytes obtained from control and diabetic rats. **(A)** Representative recordings of intracellular fura-2 ratio and sarcomere length during field stimulation. Myocytes were superfused with normal Tyrode's solution (1.8 mM Ca^{2+}). Myocyte contraction was elicited by field stimulation at 1 Hz frequency. **(B)** Averaged instance of spontaneous contraction in ventricular myocytes. Four to six myocytes were tested from each animal and data averaged to represent that animal. Data represent means \pm SE for control rats (CTL, $n = 12$), control rats treated with bosentan (CTL+B, $n = 9$), diabetic rats (STZ, $n = 9$), and diabetic rats treated with bosentan (STZ+B, $n = 8$). *represents significantly different from the control values and +represents significantly different from values taken from the non-treated diabetic rats ($p < 0.05$).

lation of ET-1 and ET-receptor expression has also been observed in the heart of diabetic rats (1,13). Treatment of diabetic animals with ET-receptor antagonists restored diabetes-induced mechanical and structural dysfunction in cardiovascular system (1,13,16,29,30). Similarly, elevated ET-1 system in diabetic patients and animals may also be responsible for diabetes-induced changes in cardiac electrophysiology. Previous study by Szokodi et al. (31) reported that in anesthetized open-chest dogs, intrapericardial infusion of ET-1 increased Q-T time and monophasic action potential duration, and induced ventricular arrhythmias. In another study, Filippo et al. (32) reported that perfusion of isolated rat hearts with high concentration of glucose sig-

nificantly prolonged the Q-T interval and increased cardiac ET-1 levels. Perfusion of the hearts with the ET receptor antagonists reduced the high glucose-induced Q-T prolongation. In the present study, in vivo treatment of diabetic rats with ET-1 receptor antagonist, bosentan, reversed diabetes-induced action potential prolongation and depression of outward K^+ currents in ventricular myocytes. These values of myocyte action potential and K^+ currents in bosentan-treated diabetic rats were no longer significantly different from that in time-matched control rats. In addition, bosentan treatment significantly lowered the occurrence of arrhythmic contraction observed in ventricular myocytes obtained from diabetic rats. On the other hand, bosentan treatment of control rats had no detectable effect on the electrophysiological parameters and cell contraction in isolated ventricular myocytes. Our data did not delineate the cellular mechanisms underlying ET-1-induced electrical instability in diabetic hearts. However, studies by others suggested a possible correlation of ET-1 elevation with oxidative stress (33), and oxidative stress is involved in the etiology of diabetes-induced downregulation of I_{to} in rats (22). ET-1 also was reported to inhibit I_{k} in guinea pig ventricular myocytes through a pertussis toxin-sensitive mechanism (34). In a *Xenopus* oocyte expression system, the transient outward K^+ currents (I_{to}) encoded by expressed Kv1.4 and Kv4.3 were decreased by stimulation of co-expressed ET-A receptor with ET-1. Reduction of I_{to} by ET-1 was associated with the channel phosphorylation by activated PKC (35). Thus, activation of PKC may be responsible for the ET-1 induced alteration of Kcurrents during diabetes development.

In summary, our study is the first to provide evidence at the cellular level that enhanced ET-1 plays an important role in the development of cardiac electrical instability observed in diabetic rats. Our data demonstrated the beneficial effects of ET-1 receptor blockade on the diabetes-induced alteration of cardiac electrophysiology, and thus suggest that ET-1 blockade may be a potential therapeutic target for diabetic cardiomyopathy. Further studies are needed to determine the cellular mechanisms underlying ET-1 induced electrical instability in diabetic hearts, as well as the acute effect of bosentan on the diabetes induced ventricular electric instability.

Material and Methods

Induction of Diabetic Rats

Male Wistar rats (230–270 g) were injected intravenously with a single dose of freshly prepared streptozotocin (STZ, 50 mg/kg; 0.05 M citrate buffer; pH 4.5) or the same volume of citrate buffer only (control) via the tail vein. STZ-injected and control rats were further divided randomly into bosentan-treated and untreated groups. Bosentan was mixed in gum Arabic (5%), prepared daily, and delivered via daily oral gavage at a dose of 100 mg/kg starting at 1 wk following STZ or saline injection. The untreated animals were

administrated gum Arabic (5%) as vehicle via daily gavage. Animal body weight was recorded daily. Plasma glucose level was determined using Accu-Chek (Roche, Indianapolis, IN) in tail vein blood collected from fed animals 72 h and 8 wk following STZ or saline injection. Animals with a glucose level of >300 mg/dL were considered diabetic. All the animals injected with STZ had glucose levels greater than 300 mg/dL and were included in our study. All the procedures of animal handling and use were approved by Auburn University Institutional Animal Care and Use Committee.

Ventricular Myocyte Isolation

Viable left ventricular myocytes were isolated from rats 8 wk following induction of diabetes using previously described methods (17). This time point (8 wk post-STZ) was chosen because our previous studies demonstrated a clear contractile dysfunction and K^+ current depression in ventricular myocytes 8 wk after STZ injection (17,36). Briefly, rats were sacrificed with decapitation, the heart rapidly removed by thoracotomy, and then mounted onto a water-jacketed Langendorff perfusion apparatus (37°C) via aortic cannula. The heart was perfused in a retrograde fashion with Ca^{2+} -free and oxygenated (100% O_{22}) Tyrode's solution for 5 min, followed with the Tyrode's solution containing 0.3 mg/mL collagenase (Type II, 371 U/mg) and 30 μM $CaCl_2$ for 10–15 min. Left ventricle was isolated and mechanically dispersed in Kraftbrühe (KB) solution. Isolated myocytes were centrifuged and resuspended in KB solution with increasing millimolar concentrations of Ca^{2+} to yield Ca^{2+} -tolerant cells. This procedure consistently yielded 40–50% rod-shaped and Ca^{2+} -tolerant ventricular myocytes from both control and STZ-injected rats. For all experiments, only rod-shaped myocytes with clear striations and no membrane blebs were used. There are no physical difference between myocytes from control and STZ-injected rats. Myocytes were stored in KB solution (1.0 mM Ca^{2+}) for 1 h at room temperature before the experiment and used within 8 h.

Measurement of Membrane Potentials and Currents

Membrane potentials and currents were recorded in ventricular myocytes using the whole-cell patch-clamp technique (37). Patch pipettes were prepared from borosilicate glass with a PE-830 pipette puller (Narishige, Japan) and polished with a MF-830 microforge (Narishige, Japan). The pipette resistance was 2–4 M Ω when filled with the appropriate pipette solution. After the whole-cell configuration, capacity transients and series resistance are measured by a 20-mV hyperpolarizing potential and partially compensated. Membrane potentials and currents of myocytes were measured via an Axopatch 200B patch-clamp amplifier (Axon, CA). Voltage-clamp protocols were applied to the cells using the data acquisition package pClamp 9 (Axon, CA) and filtered at 5 kHz. All the experiments were performed at room temperature ($25 \pm 1^\circ C$).

Action potential was recorded using current-clamp mode when myocytes were superfused with normal Tyrode's solution. Action potential was elicited by a 6-ms current pulse (30% above threshold) at a 30-s interval. Resting membrane potential, amplitude of action potential, and times to 50% (APD50) and 90% repolarization (APD90) were recorded and analyzed.

Inward L-type Ca^{2+} currents were recorded in the voltage-clamp mode. Inward current was elicited by stepping voltage from the holding potential of -40 mV to $+10$ mV at 30 s intervals.

Outward K^+ currents were recorded in the voltage-clamp mode. I_{to} was recorded in the presence of external tetraethylammonium chloride (TEA-Cl, 50 mM). The resting membrane potential was held at -60 mV. Current was elicited by test pulses between -30 and $+50$ mV applied in 10 mV increments at a frequency of 0.1 Hz. Values were corrected by subtracting the TEA-resistant I_{ss} . I_k was recorded in the presence of 4-aminopyridine (4-AP, 5 mM). The resting potential was held at -120 mV. A prepulse to -40 mV (15 ms) was applied to inactivate I_{Na} , followed by test pulses between -30 and $+50$ mV (10 mV increments) at a frequency of 0.05 Hz. I_{ss} was recorded in the absence of TEA and 4-AP. The holding potential was set at -20 mV to inactivate I_{Na} , I_{to} , and I_k . The test pulses between -30 to $+50$ mV were applied at a frequency of 0.1 Hz.

Measurement of Myocyte Contraction and Intracellular Ca^{2+} Concentration

Cardiac myocyte contraction and intracellular Ca^{2+} transient ($[Ca^{2+}]_i$) were recorded simultaneously using fura-2 fluorescence and edge detection system (IonOptix, MA, USA). Briefly, myocytes were loaded with fura-2/AM (2.5 μM) at room temperature (approx $22^\circ C$) for 20 min and then washed twice with fura-2-free Tyrode's solution. Fura-2-loaded myocytes were placed in a cell perfusion chamber mounted on an inverted microscope (Nikon TE 2000) and perfused with normal Tyrode's solution by gravity (approx 2 mL/min) at room temperature. Myocyte contraction was elicited at 1 Hz frequency by field stimulation with two platinum electrodes on both sides of the cell perfusion chamber. Intracellular fura-2 fluorescence was excited with a collimated light beam from a 150-W xenon arc lamp. An adjustable rectangular diaphragm restricted recording to one cell in the field of view. The emitted fluorescence passed to a spectrophotometer and was converted to voltage. The signals were then digitized via an analog-to-digital converter (IonOptix, MA) for data storage and subsequent analysis.

Chemicals and Solutions

STZ and all the chemicals were purchased from Sigma (Sigma, St. Louis, MO). Bosentan was a generous gift from Dr. Martine Clozel (Acetelion, Switzerland).

Tyrode's solution was composed of (in mmol/L): 137 NaCl, 5.4 KCl, 4.4 $NaHCO_3$, 1.5 KH_2PO_4 , 1.0 $MgCl_2$, 1.8

CaCl₂, 10 HEPES, and 10 glucose (pH 7.4). KB solution was composed of (in mmol/L): 25 KCl, 70 L-glutamic acid, 1.0 MgCl₂, 10 KH₂PO₄, 1.0 EGTA, 10 HEPES, 10 glucose, 10 taurine, 10 DL-β-hydroxybutyric acid, and 1 mg/mL albumin (pH 7.4).

The pipette solution for action potential recording was (in mmol/L): 100 KCl, 10 NaCl, 5.0 ATP-Mg, 10 EGTA, 2.0 MgCl₂, 10 HEPES, 5.5 glucose, 0.5 GTP-Mg, pH is adjusted to 7.2 with KOH.

For I_{Ca,L} measurements, the pipette solution contained (in mmol/L) 10 ethylene glycol-bis(β-aminoethyl ether)-N,N,N',N'-tetraacetic acid (EGTA), 10 HEPES, 2 MgCl₂, 5 MgATP, 0.1 GTP, 20 tetraethylammonium chloride (TEA-Cl), 85 CsCl, and 5.5 glucose (pH adjusted to 7.2 with CsOH). The bath solution was composed of (in mmol/L): 137 NaCl, 1.8 CaCl₂, 1.0 MgCl₂, 10 glucose, 5.4 CsCl, 10 HEPES, pH 7.40 with NaOH. K⁺ currents were eliminated by adding TEA-Cl in both bath and pipette solutions. Na⁺ channels and T-type Ca²⁺ channels were inactivated by holding the membrane potential at -40 mV.

For K⁺ current recordings the bath solution was composed of (in mmol/L): 137 NaCl, 4 KCl, 1 MgCl₂, 10 HEPES, 0.5 CaCl₂, 10 glucose, pH adjusted to 7.4 with NaOH. When 4-AP is added to the solution, pH is readjusted to 7.4 with HCl. When TEA-Cl was added to the solution, NaCl was equimolarly substituted by TEA-Cl. The pipette solution for K⁺ current recording was (in mmol/L): 80 L-aspartic acid, 50 KCl, 10 KH₂PO₄, 1 MgSO₄, 5 HEPES, 3 ATP_{Na}, 10 EGTA, pH adjusted to 7.4 with KOH.

Statistical Analysis

Experiments were performed on three to six myocytes from the same animal for each protocol and data were averaged to represent that animal. Values were reported as mean ± SEM and *n* as the number of animals studied. Data from different groups of cells were compared using two-tailed unpaired and paired Student's *t*-test, and two-way ANOVA with a Student-Newman-Kuels post test, whenever appropriate. *p* value < 0.05 is considered significantly different.

Acknowledgments

This study was partially supported by research grants from AHA Southeast Affiliation (0255030B, J. Zhong) and Auburn University Biogrant program (J. Zhong).

References

- Hileeto, D., Cukiernik, M., Mukherjee, S., et al. (2002). *Diabetes Metab. Res. Rev.* **18**, 386–394.
- Chen, S., Evans, T., Mukherjee, K., Karmazyn, M., and Chakrabarti, S. (2000). *J. Mol. Cell Cardiol.* **32**, 1621–1629.
- Malhotra, A., Penpargkul, S., Fein, F. S., Sonnenblick, E. H., and Scheuer, J. (1981). *Circ. Res.* **49**, 1243–1250.
- Zhang, X., Ye, G., Duan, J., Chen, A. F., and Ren, J. (2003). *Endocr. Res.* **29**, 227–236.
- Casis, O., Gallego, M., Iriarte, M., and Sanchez-Chapula, J. A. (2000). *Diabetologia* **43**, 101–109.
- Nobe, S., Aomine, M., Arita, M., Ito, S., and Takaki, R. (1990). *Cardiovasc. Res.* **24**, 381–389.
- Jourdon, P. and Feuvray, D. (1993). *J. Physiol.* **470**, 411–429.
- Shimoni, Y., Hunt, D., Chuang, M., Chen, K. Y., Kargacin, G., and Severson, D. L. (2005). *J. Physiol.* **567**, 177–190.
- Pacher, P., Ungvari, Z., Nanasi, P. P., and Kecskemeti, V. (1999). *Acta Physiol. Scand.* **166**, 7–13.
- Robillon, J. F., Sadoul, J. L., Benmerabet, S., Joly-Lemoine, L., Fredenrich, A., and Canivet, B. (1999). *Diabetes Metab.* **25**, 419–423.
- Magyar, J., Iost, N., Kortvely, A., et al. (2000). *Pflugers Arch.* **441**, 144–149.
- Shimoni, Y., Severson, D., and Giles, W. (1995). *J. Physiol.* **488**, 673–688.
- Chen, S., Evans, T., Mukherjee, K., Karmazyn, M., and Chakrabarti, S. (2000). *J. Mol. Cell Cardiol.* **32**, 1621–1629.
- Erbas, T., Erbas, B., Kabakci, G., Aksoyek, S., Koray, Z., and Gedik, O. (2000). *Clin. Cardiol.* **23**, 259–263.
- Makino, A. and Kamata, K. (1998). *Br. J. Pharmacol.* **123**, 1065–1072.
- Verma, S., Arikawa, E., and McNeill, J. H. (2001). *Am. J. Hypertens.* **14**, 679–687.
- Ding, Y., Zou, R., Judd, R. L., Schwartz, D. D., and Zhong, J. (2006). *J. Cardiothorac-Ren. Res.* **1**, 23–32.
- Nerbonne, J. M. and Kass, R. S. (2005). *Physiol. Rev.* **85**, 1205–1253.
- Rana, B. S., Band, M. M., Ogston, S., Morris, A. D., Pringle, S. D., and Struthers, A. D. (2002). *Am. J. Cardiol.* **90**, 483–487.
- Landstedt-Hallin, L., Englund, A., Adamson, U., and Lins, P. E. (1999). *J. Intern. Med.* **246**, 299–307.
- El-Atat, F. A., McFarlane, S. I., Sowers, J. R., and Bigger, J. T. (2004). *Curr. Diab. Rep.* **4**, 187–193.
- Xu, Z., Patel, K. P., Lou, M. F., and Rozanski, G. J. (2002). *Cardiovasc. Res.* **53**, 80–88.
- Wang, D. W., Kiyosue, T., Shigematsu, S., and Arita, M. (1995). *Am. J. Physiol.* **269**, H1288–H1296.
- Shimoni, Y. and Liu, X. F. (2003). *J. Physiol.* **550**, 401–412.
- Pierce, G. N. and Russell, J. C. (1997). *Cardiovasc. Res.* **34**, 41–47.
- Nishiyama, A., Ishii, D. N., Backx, P. H., Pulford, B. E., Birks, B. R., and Tamkun, M. M. (2001). *Am. J. Physiol.* **281**, H1800–H1807.
- Takahashi, K., Ghatei, M. A., Lam, H. C., O'Halloran, D. J., and Bloom, S. R. (1990). *Diabetologia* **33**, 306–310.
- Hopfner, R. L., McNeill, J. R., and Gopalakrishnan, V. (1999). *Eur. J. Pharmacol.* **374**, 221–227.
- Evans, T., Deng, D. X., Chen, S., and Chakrabarti, S. (2000). *Diabetes* **49**, 662–666.
- Chen, S., Evans, T., Deng, D., Cukiernik, M., and Chakrabarti, S. (2002). *Nephron* **90**, 86–94.
- Szokodi, I., Horkay, F., Merkely, B., et al. (1998). *Cardiovasc. Res.* **38**, 356–364.
- Gross, M. L., Heiss, N., Weckbach, M., et al. (2004). *Diabetologia* **47**, 316–324.
- Kahler, J., Mendel, S., Weckmuller, J., et al. (2000). *J. Mol. Cell Cardiol.* **32**, 1429–1437.
- Washizuka, T., Horie, M., Watanuki, M., and Sasayama, S. (1997). *Circ. Res.* **81**, 211–218.
- Hagiwara, K., Nunoki, K., Ishii, K., Abe, T., and Yanagisawa, T. (2003). *Biochem. Biophys. Res. Commun.* **310**, 634–640.
- Ding, Y., Zou, R., Judd, R. L., and Zhong, J. (2006). *Endocrine* **29**, 135–141.
- Zhong, J., Hwang, T. C., Adams, H. R., and Rubin, L. J. (1997). *Am. J. Physiol.* **273**, H2312–H2324.